Hysteresis Model of Contraction Pneumatic Muscle Actuator

Huda Al-Qurnawi and Alaa Al-Ibadi

ABSTRACT

Pneumatic muscle actuator (PMA) is a type of linear pneumatic actuator that is soft and flexible, capable of moving like human muscles. These characteristics allow the muscle actuators to adapt to different robotic systems and medical applications. This paper presents the design, construction, characterization, and experimental validation of PMA. In addition to describing the pneumatic muscle contraction, the significant hysteresis nonlinearities of PMAs have hampered high-precision motion control. This paper presents new forma for modeling the length of the contraction PMA. Because contraction length parameters have a sigmoidal structure, the sigmoid function is a suitable form to model. Applied the fitting curve method. We use the MATLAB function lsqcurvefit to fit the equation to the data. The mathematical model was validated with Mean Squared Error (MSE) between the experimental results and the mathematical model. additionally, computed the correlation coefficient to assess the relationship between the model predictions and the experimental data.

Keywords: Contraction pneumatic muscle actuator, Hysteresis modeling, Sigmoidal length-pressure model, MATLAB curve fitting, Soft rehabilitation robotics

Department of Computer Engineering, Engineering College, University of Basrah, Basrah, Iraq

Correspondence to: Huda Al-Qurnawi, pgs.huda.ali24@uobasrah.edu.iq

Additional material is published online only. To view please visit the journal online.

Cite this as: Al-Qurnawi H and Al-Ibadi A. Hysteresis Model of Contraction Pneumatic Muscle Actuator. Premier Journal of Science 2025;15:100212

DOI: https://doi.org/10.70389/PJS.100212

Peer Review

Received: 14 August 2025

Last revised: 7 November 2025

Accepted: 17 December 2025

Version accepted: 6

Published: 8 January 2026

Ethical approval: N/a

Consent: N/a

Funding: No industry funding

Conflicts of interest: N/a

Author contribution: Huda Al-Qurnawi and Alaa Al-Ibad– Conceptualization, Writing – original draft, review and editing

Guarantor: Huda Al-Qurnawi

Provenance and peer-review: Unsolicited and externally peer-reviewed

Data availability statement: N/a

Introduction

Robots are increasingly assisting humans, especially the elderly and disabled. However, building rigid robotic joints becomes more complex when trying to match the softness of human arms and flexible joints, which are moved by many muscles. Researchers inspired by the need for human-like actuator systems developed the pneumatic muscle actuator (PMA). The mechanism moves as a result of the PMA's conversion of pneumatic power into pulling force. The performance characteristics of these systems are comparable to and more robust than those of human muscle.[1–3] Soft robots are robots composed of elastic, moldable materials like soft plastic, silicone, and rubber. These robots imitate living things like octopuses, worms, fish, and even certain plants using designs influenced by nature. Soft robots can bend, stretch, and compress without suffering damage, making them versatile and able to adapt to diverse settings.[4–7]

Soft robots possess desired traits Because of their consistently deformable and compliant structures, which can tolerate large deformations during normal operation these features include like conformability to their surroundings embedded in their mechanical constructions, but their flexibility and compliance make accurate, high-bandwidth control more difficult than their rigid counterparts. Therefore, researchers are increasingly developing soft robots for applications in crowded and unstructured environments, including manipulation, search and rescue operations, and human-centered jobs.[8–11]

PMA are more secure than other devices that use heat, electricity, or chemically active materials because they can be made from inexpensive materials that are readily available, have high degrees of freedom due to the soft actuator's ability to bend, are inexpensive because they can be made from readily available compressed air, have a lifting force of 6000 N despite only weighing about 800 grams, and have high strength relative to volume that is five times greater than that provided by electric motors.[12,13]

And having very comparable compliance to muscles. Because of these features It is commonly utilized in arm/ankle orthotics, elbow exoskeleton lower-limb rehabilitation, and medical nursing.[14] Although PMAs offer many benefits, they also have a number of drawbacks that might restrict their use. For the most part, these PMAs exhibit hysteretic behavior due to the friction between the braided sleeves' wires, and because there is inherent friction, the muscle's temperature rises over time during operation, significantly affecting its dynamic properties. A rise in temperature can accelerate material fatigue, modify the inner tube's viscoelastic response, and affect the air's compressibility. These changes can lead to performance drift and less repeatability in the actuator's behavior. Additionally, they exhibit nonlinear behavior due to the viscoelastic properties of the inner tubes, the compressibility of the air inside, and the geometrically complex behaviors of the PMA outer covering, and hysteresis causes a change in the way the muscle reacts to pressure changes, which means that depending on whether the muscle is in the process of inflating or deflating, the force it exerts for a given pressure may vary. Because of this, it is more difficult to attain accurate control, particularly in applications that need precise force or location. However, building a precise dynamic model of PMA may successfully resolve the aforementioned issues.[15–17]

Currently, modeling and hysteresis compensation are gradually emerging as important study topics. From a mathematical perspective, we can easily divide the PMA's dynamic models into two categories: physics-based models and phenomenon-based models. The physics-based model mostly figures out how the PMA's shape and material properties relate to the thickness of the rubber tubes so that a static model of the PMA can be made using the force balance method. Physics-based models include many model parameters and complex mathematical derivations, which make controller design very challenging and raise

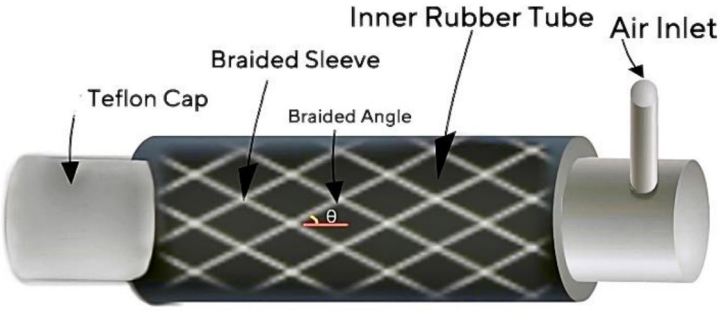

Fig 1 | Structure of pneumatic muscle actuator

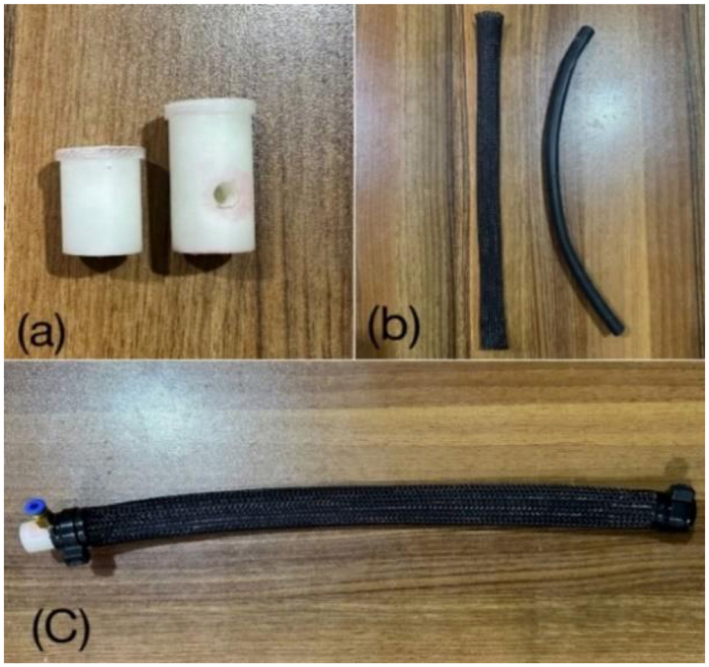

Fig 2 | Photo of PMA (a) Teflon caps (b) Sleeve and rubber tube (c) 30 cm PMA

Fig 3 | PMA is at rest and pressurized

processing costs significantly. Alternatively, we create phenomenon-based models using reduced model descriptions and experimental data.[18,19]

Structure of PMA and Material

The contraction-type PMA is designed from a rubber tube surrounded by a braided sleeve that has two ends made of plastic (or any solid material). Figure 1 shows the structure of the contractor muscle. The braided mesh represents the length of the PMA, which is similar to the rubber tube length. The PMA produces its contraction performance when the angle θ is less than 54.7°. Although it varies from muscle to muscle, the contraction ratio never exceed 30%.[20]

The intended pneumatic muscle for contraction consists of a braided sleeve of 35.5 cm in length and 1.6 cm in diameter. The inner tube is rubber used by bicycles. It is simple to use, and its material structure allows it to expand and contract. The tube length is 35.5 cm and 1.6 cm in diameter, and the muscle length is 30 cm and 1.8 in diameter.

Two cylinders of Teflon caps were applied to either end of the muscle. The first one is 3.5 cm long and has a 2 cm diameter with an air-passing hole inside. The second one is 2.5 cm long and has a comparable diameter. Which are tightly held using cable ties.

The braided sleeve fully encased the rubber tube, and the covers are fastened to the tube with tape and a water cap to prevent them from moving when air was pumped into the tube. show in Figure 2.

When compressed air is pumped into the rubber tube's interior, it expands radially and contracts in length. The inner netting serves as a spring to return the tube's natural shape as air leaves it show Figure 3.[21]

Experiment and Testing of PMA

It's been completed conducted several experiments to measure the length of the muscle. Changes in muscle length were observed with a change in pressure applied to it. The aim of these experiments was to understand the behavior of the muscle during contraction and relaxation. The experiments are performed as follows:

- Fix the PMA vertically on the frame.
- Connect distance tracking (ultrasonic) sensor to the free end to measure distance.
- Use a pressure sensor to measure the air pressure.
- Use an Arduino Mega 2560 to control the experiment process.
- The free end of the PMA holds the ultrasonic sensor, and a screw secures the other end.
- Apply air pressure via the valve. Measure the distance readings at various pressure levels to analyze the muscle's response.

See Figure 4 for the equipment used in the experiment.

The experiment is carried out as follows: The experiment begins with the muscle at its natural length of 30 cm. Next, we apply air pressure ranging from (0–500) kPa. Pressures above 500 kPa may cause harm to humans. Furthermore, muscle movement is relatively

DOI: https://doi.org/10.70389/PJS.100212 | Premier Journal of Science 2025;15:100212

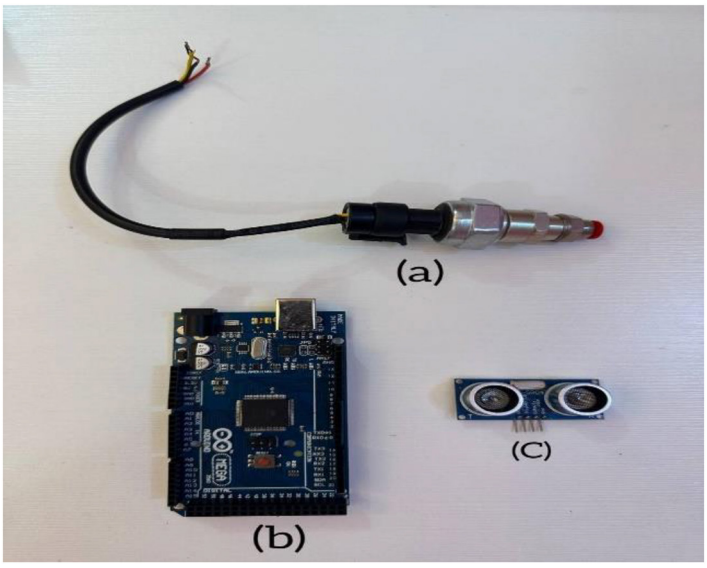

Fig 4 | The devices used in the experiment (a) pressure sensor (b) Arduino Mega 2560 (c) ultrasonic sensor

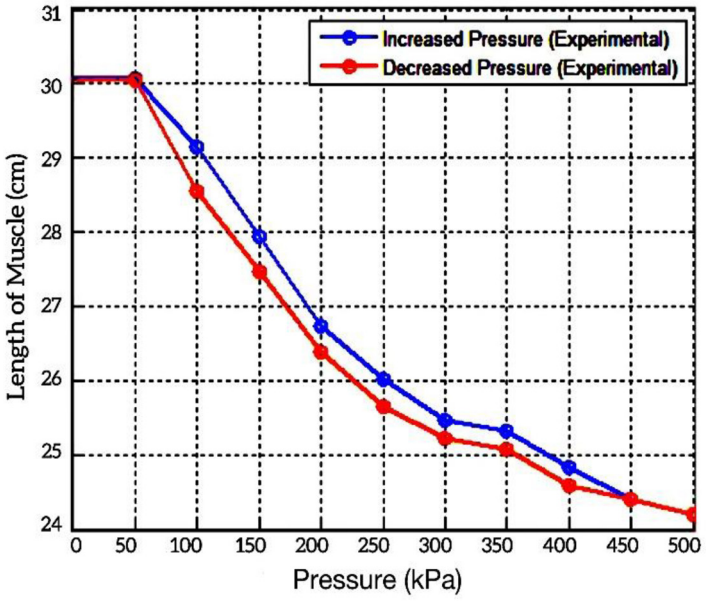

Fig 5 | PMA length during increased and decreased pressure experiments

Table 1 | Pressure in relation to length during an increase and decrease

Pressure (kPa)	Length Increased Pressure (cm)	Length Decreased Pressure (cm)
0	30.06	30.06
50	30.06333333	30.05666667
100	29.14	28.54666667
150	27.94333333	27.46333333
200	26.74	26.38
250	26.00666667	25.64333333
300	25.47	25.22666667
350	25.32333333	25.08333333
400	24.82	24.59333333
450	24.4	24.39
500	24.2	24.2

stable between (450 and 500) kPa, so there is no need for higher pressures. This pressure causes the muscle to contract, causing its length to decrease until it reaches 24 cm at a pressure of 500 kPa. In the second stage, we decrease the air pressure from (500–0) kPa, allowing the muscle to return to its natural size. Sensor calibration is rest at each experiment set to zero. By analyzing the collected data, Figure 5 illustrates the pressure and length curves, as well as the muscle's behavior and response to pressure changes. The numerical results are displayed in the Table 1, which are an average of several conducted experiments.

The blue curve illustrates the muscle's length change behavior under increasing pressure, while the red curve illustrates the muscle's behavior under decreasing pressure.

Observe that at the beginning, when the pressure is between 0 and 50, the resistance of the materials that make up the muscle, such as the rubber tube and sleeves, prevents any change in the muscle's length because the applied pressure is insufficient.

Since the muscle's materials are not elastic, it requires a certain amount of pressure to expand and contract, so length doesn't change.

Then, when the pressure increases, the muscle undergoes a significant change in length because it has reached a sufficient pressure to resist the flexibility and friction of the materials that make up the muscle. Moreover, the muscle tends to exhibit exponential behavior. And once the pressure reaches 400, the length stabilizes as the sleeve's diameter reaches its maximum value.

It can be observed that the muscle length shows a different behavior when the pressure increases compared to when the pressure decreases. During the extension and contraction cycles, there is a noticeable slowdown, which shows that the muscle does not respond in a straight line. This is because of the hysteresis phenomenon, which is caused by the interaction of several factors, including the internal friction of the fibers and the rubber tube and the variation between the pressure inside the muscle and the air pressure outside.

Calibration of Sensors

Sensor of Distance

The HC-SR04 ultrasonic sensor is a low-cost distance measurement device that operates based on ultrasonic time-of-flight. It transmits a 40 kHz pulse and measures the echo return time to calculate distance, with a measurement range of 2–400 cm and an accuracy of approximately ±3 mm. Due to its simplicity, real-time response, and ease of interfacing with microcontrollers, it is widely used in robotic applications and distance monitoring systems.[22]

Pressure Sensor

An analog industrial pressure sensor was used to measure the internal pressure of the pneumatic muscle during operation. Operating within a range of 0–0.5 MPa (0–500 kPa), the sensor provides a linear signal from 0.5 to 4.5 V, proportional to the pressure value,

when supplied with 5 V. This type of sensor is robust and stable, making it suitable for both pneumatic and mechanical applications. Its accuracy is approximately ±2% of the entire measurement range, or about ±10 kPa, with a total uncertainty of approximately ±20 kPa. This accuracy is sufficient for pneumatic muscle testing, monitoring, and real-time pressure control.

Modelling

To determine the relationship between the length and pressure of the pneumatic muscle, several authors have tried to create a mathematical model that depicts the behavior of the actuator.[21] An accurate and important mathematical model is created based on how muscle length changes under pressure, which resembles the shape of the sigmoid function, so the sigmoid function was chosen to represent the mathematical model. Researcher Alaa Al-Abbadi employs this method.[23] General Equation for sigmoid. Where the length of the pneumatic muscle actuator (PMA) as a function of applied pressure is modeled using the following equation:

$$L = L_0 - \frac{aL_0}{\left(1+e^{-bP}\right)^{6.214}} \quad (1)$$

Where:

To find the best fit between the model and experimental data, the exponent (6.214) was determined by iteratively adjusting its value and performing curve fitting to experimental data. Due to the highly nonlinear behavior of pneumatic muscles, analytical determination was not feasible, so trial-and-error was used to minimize fitting error and accurately match the real muscle response.

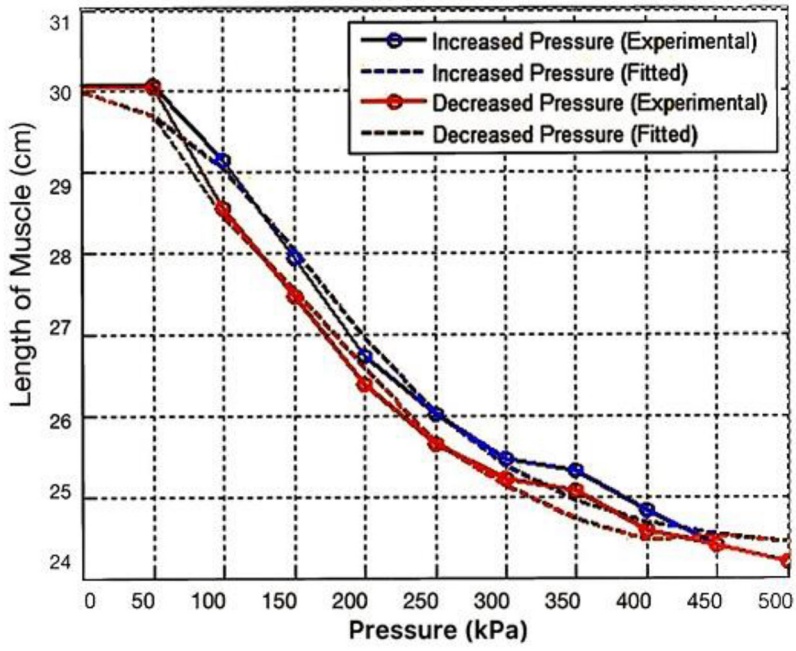

Fig 6 | Hysteresis in pneumatic muscle actuator

As a result, a collection of equations was established. used the fitting curve approach to model the system in (2). This method is among the simplest ways to identify a system, whether it be dynamic or static.[24]

Used MATLAB's lsqcurvefit function to fit the parameters a and b of the model. The fitting procedure uses the experimental data of muscle length in a relation of pressure. The function minimizes the difference between the experimental data and the theoretical model by adjusting the parameters a and b. The curve fitting function has the following form:

$$L_{fitting} = L_0 - \frac{aL_0}{\left(1+e^{-bP}\right)^{6.214}} \quad (2)$$

Where:

- A and b are the fitting parameters determined by the fitting process.
- P is the applied pressure, which is given as data.

In (3) To account for the hysteresis, we introduce a second relationship for the length of the muscle when pressure is decreasing. This model incorporates a hysteresis term, which is the difference between the muscle length at increasing and decreasing pressures.

$$\Delta L_{hysteresis} = L_{increasing}(P) - L_{decreasing}(P) \quad (3)$$

The model for the decreasing pressure can be expressed as:

$$L_{decreasing}(P) = L_{increasing}(P) - \Delta L_{hysteresis}$$

Where:

- $\Delta L_{hysteresis}$ is the difference in muscle length between the increasing and decreasing pressure conditions.
- $L_{increasing}(P)$: Length during increasing pressure.
- $L_{decreasing}(P)$: Length during decreasing pressure.

Result

In this section, the results of the mathematical model presented in the modeling section will be compared with experimental data in order to confirm the validity of the model. The following diagrams will illustrate the relationship between the specified factors, such as length and pressure.

Figure 6 shows the connection between the pneumatic muscle's length and the pressure applied, discussed earlier, to illustrate the experimental data during pressure increases and decreases. A curve fitting technique was used to improve the agreement between the experimental data and the theoretical data.

When using MATLAB's lsqcurvefit function, the code modifies a and b to make the predicted length function as close to the real length data as possible. To decrease the error (difference) between the experimental and anticipated values.

DOI: https://doi.org/10.70389/PJS.100212 | Premier Journal of Science 2025;15:100212

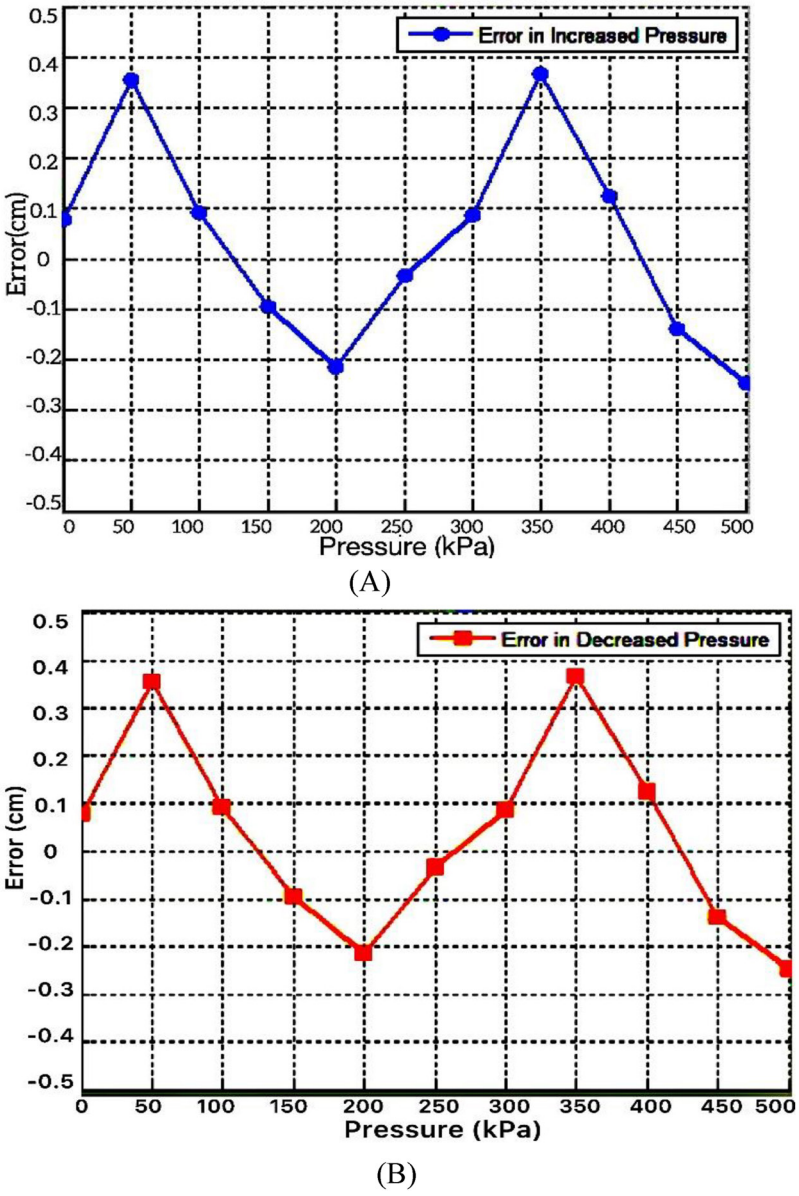

Fig 7 | The error difference between the experimental data and the mathematical model data, (A) Error in Increased Pressure, (B) Error in Decreased Pressure

Table 2 | Comparison of sigmoid and Bouc–Wen models

Path	Model	MAE	MSE	R^2	AIC	BIC
Increasing	Sigmoid	0.1664	0.1578	0.9912	−31.5628	−30.7670
	Bouc–Wen	0.4247	0.2656	0.9404	−2.5674	−0.1800
Decreasing	Sigmoid	0.1664	0.1578	0.991	−31.5628	−30.7670
	Bouc–Wen	0.4179	0.2663	0.9392	−2.5725	−0.1851

Table 3 | Symbols description

Symbols	Description	Unit
L	is the length of the muscle at pressure P.	cm
L_0	is the initial length of the muscle.	cm
a and b	are fitting parameters that need to be determined.	dimensionless
P	is the applied pressure.	kPa
6.214	is a scaling factor that improves the accuracy of the model.	dimensionless constant

Where:

Fitted value for a= 0.19073.
Fitted value for b= 0.011333.

The blue dotted curve represents curve fitting when pressure increases, while the red dotted curve represents curve fitting when pressure decreases. The gap between them represents hysteresis, the non-linear behavior of a pneumatic muscle.

The analysis of the proposed model showed that it provides excellent accuracy, as there is a clear match between the experimental and theoretical values at most points with a slight deviation. calculated the mean square error (MSE) and the correlation coefficient Using MATLAB, finding that the MSE was 0.15776, indicating a low level of error. found the correlation coefficient when increased pressure to be 0. 99603. The correlation coefficient when decreased pressure is 0.99598. These numbers indicate a high strength of agreement between the experimental data and the mathematical model.

The Mean Absolute Error (MAE) was 0.16642 for both increasing and decreasing pressure. The coefficient of determination (R^2) was 0.99115 for increasing pressure and 0.991 for decreasing pressure, demonstrating the high accuracy of the proposed model.

Figure 7 shows the error difference between the mathematical model data and the experimental data, where (A) represents the error in the case of increasing pressure, while (B) represents the error in the case of decreasing pressure. can analyze the results in the following way: The model accurately represents the experimental values when the error is close to zero. However, when the error goes beyond zero towards positive values, it signifies that the experimental values surpass the theoretical values. In other words, the model assumes that the muscle length is shorter than its actual length. And when the error value is negative, the model assumes that the muscle length is longer than its original length. This error is because of the behavior of the muscle material.

Comparison of Sigmoid and Bouc–Wen Models

The Sigma method and the Bouc-Wen model were compared using the same experimental dataset to evaluate the performance of the proposed models. The coefficient of determination (R^2), mean square error (MSE), and mean absolute error (MAE) were used as the main statistical indicators for comparison. Table 2 below illustrates these differences.

The sigmoid model, which more smoothly and simply captured the nonlinear muscle action, generally demonstrated a closer alignment with the experimental data. Although the Bouc–Wen model was effective at depicting hysteresis in general, it tended to overstate the loop area and produced a less accurate fit. The sigmoid method turned out to be the more accurate and trustworthy way to depict the behavior of the actuator in this situation.

Figure 8 plots the experimental findings against the two models to provide a visual comparison. The Bouc–Wen curve exhibits pronounced deviations and

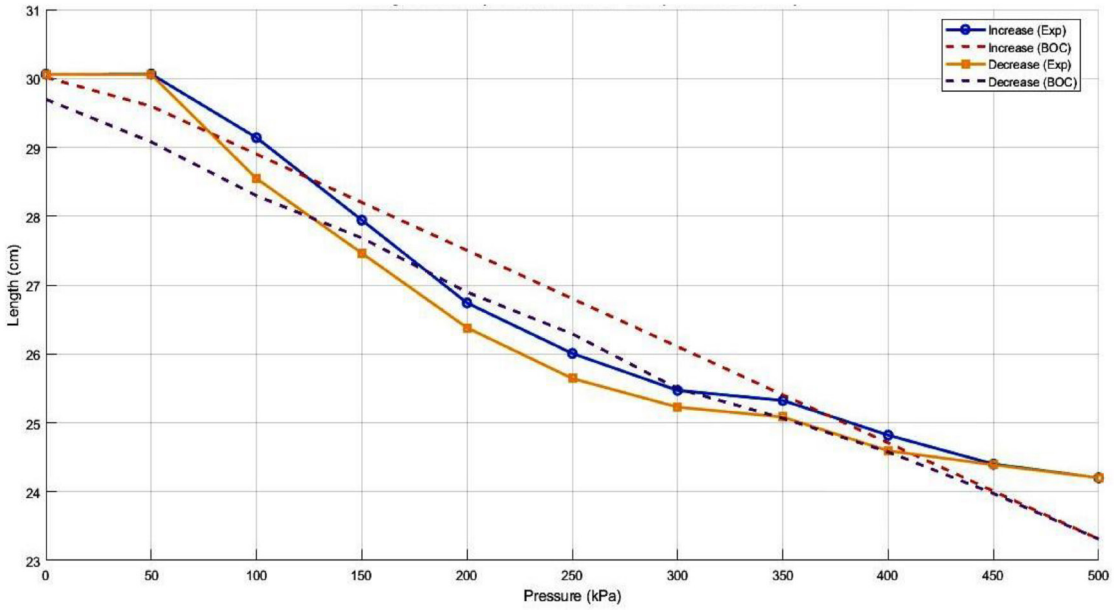

Figure 8 | Sigmoid and Bouc-Wen model predictions are compared with experimental data

a greater hysteresis loop area, whereas the sigmoid curve more closely reflects the experimental trend. The statistical results shown in Table 3 are supported by this visual evidence.

Conclusion

This study investigated the contractile behavior of pneumatic muscle actuators (PMAs) using both mathematical modeling and experimental methods. Muscle length was measured in laboratory tests under different applied pressures.

One of the most important findings was the presence of hysteresis, which had a significant effect on muscle length as pressure increased and decreased. Different contraction and relaxation trajectories illustrate the nonlinear behavior of the hysteresis effect in PMA. On the other hand, used a curve-fitting technique to calculate muscle length/pressure using a sigmoid function, which improved the accuracy and consistency of the theoretical model equation for muscle length with the experimental data.

The mean square error (MSE), which showed a high degree of accuracy in the model's predictions, validated the agreement between the experimental data and the suggested mathematical model. This validation demonstrates the dependability of the sigmoid function in simulating PMA contraction dynamics and Several research studies have put forth models, with differing degrees of accuracy, to forecast the behavior of pneumatic muscle actuators (PMAs). For instance, a model displayed MSE values ranging from 7.23 to 22.68, demonstrating a substantial discrepancy between theoretical and experimental outcomes.[13]

Conversely, the model in this paper shows enhanced accuracy with a significantly lower MSE of 0.15776. The study's conclusions advance the use of PMAs in domains where precise and flexible actuation is essential, such as industrial automation, robotics, and prosthetics. Further research could build on this foundation to explore real-time control techniques and improve PMA performance in dynamic operating environments. For future research, this model can be used for control systems.

Acknowledgment

I would like to express my thanks and appreciation to the Department of Computer Engineering at the University of Basrah for providing a laboratory to work in. This acknowledgement highlights the significance of institutional support in facilitating academic research. Such support not only offers monetary aid but also produces an atmosphere that is suitable to academic growth.

References

1 Najmuddin WSWA, Mustaffa MT. A study on contraction of pneumatic artificial muscle (PAM) for load-lifting. J Phys Conf Ser. 2017;908(1):012036. https://doi.org/10.1088/1742-6596/908/1/012036
2 Jørgensen J, Bojesen KB, Jochum E. Is a soft robot more 'natural'? Exploring the perception of soft robotics in human-robot interaction. Int J Soc Robot. 2022;14(1):95–113. https://doi.org/10.1007/s12369-021-00761-1
3 Al-Ibadi A, Nefti-Meziani S, Davis S. Cooperative project by self-bending continuum arms. In: Proceedings of the 23rd IEEE International Conference on Automation and Computing (ICAC). IEEE; 2017. p. 7–8. https://doi.org/10.23919/IConAC.2017.8082045
4 Al-Qurnawi H, Al-Ibadi A. Back-support exoskeletons and rehabilitation robotic systems: a review. J Robot Res. 2024;2(1):1–13. https://doi.org/10.64820/AEPJRR.21.1.13.62025
5 Al-Fahaam H, Nefti-Meziani S, Theodoridis T, Davis S. The design and mathematical model of a novel variable stiffness extensor-contractor pneumatic artificial muscle. Soft Robot. 2018;5(5):576–91. https://doi.org/10.1089/soro.2018.0010

6 Al-Ibadi A, Nefti-Meziani S, Davis S. A robot continuum arm inspired by the human upper limb: the pronation and supination rotating behaviour. In: 2020 International Conference on Electrical, Communication, and Computer Engineering (ICECCE). IEEE; 2020. p. 1–6. https://doi.org/10.1109/ICECCE49384.2020.9179338
7 Mohammed M. Types and applications of soft robot arms and end-effectors: a review. J Robot Res. 2024;1(1):40–52. https://doi.org/10.64820/AEPJRR.11.40.52.122024
8 Schmitt F, Piccin O, Barbé L, Bayle B. Soft robots manufacturing: a review. Front Robot AI. 2018;5:84. https://doi.org/10.3389/frobt.2018.00084
9 Mohsen HA, Al-Ibadi A, Abdalla TY. A variable-length, variable stiffness soft endoscope (VL-VS-SE) for upper gastrointestinal tract. J Robot Res. 2024;1(1):1–6. https://doi.org/10.64820/AEPJRR.11.1.6.122024
10 Al-Shamkhani D, Al-Ibadi A, Giannaccini ME. Soft robot for ankle rehabilitation. In: 2023 16th International Conference on Development in eSystems Engineering (DeSE). IEEE; 2023. p. 486–91. https://doi.org/10.1109/DeSE60595.2023.10468823
11 Wickramatunge KC, Leephakpreeda T. Study on mechanical behaviors of pneumatic artificial muscle. Int J Eng Sci. 2010;48(2):188–98. https://doi.org/10.1016/j.ijengsci.2009.08.001
12 Al-Mayahi W, Al-Fahaam H. A review of design and modeling of pneumatic artificial muscle. Iraqi J Electr Electron Eng. 2024;20(1):122–36. https://doi.org/10.37917/ijeee.20.1.13
13 Al-Ibadi A, Nefti-Meziani S, Davis S. Efficient structure-based models for the McKibben contraction pneumatic muscle actuator: the full description of the behaviour of the contraction PMA. Actuators. 2017;6(4):32. https://doi.org/10.3390/act6040032
14 Xie S, Mei J, Liu H, Wang Y. Hysteresis modeling and trajectory tracking control of the pneumatic muscle actuator using modified Prandtl-Ishlinskii model. Mech Mach Theory. 2018;120:213–24. https://doi.org/10.1016/j.mechmachtheory.2017.07.016
15 Saito N, Satoh T, Saga N. Double air chambers pneumatic artificial muscle and non-hysteresis position control. Actuators. 2024;13(8):282. https://doi.org/10.3390/act13080282
16 Al-Shamkhani D, Al-Farhan F, Al-Ibadi A. The wearable foot rehabilitation soft robot. In: Proceedings of the International Conference on Communication and Information and Technology (ICICT). IEEE; 2021. p. 197–201. https://doi.org/10.1109/ICICT52195.2021.9568432
17 Al-Ibadi A, Nefti-Meziani S, Davis S, Theodoridis T. Design of two segments continuum robot arm based on pneumatic muscle actuator (PMA). In: Proceedings of the 24th IEEE International Conference on Automation and Computing (ICAC). IEEE; 2018. p. 1–6. https://doi.org/10.23919/IConAC.2018.8749087
18 Ma G, Jia H, Xia D, Hao L. Hysteresis compensation and trajectory tracking control model for pneumatic artificial muscles. Appl Sci. 2024;14(21):9684. https://doi.org/10.3390/app14219684
19 Xu JH, Xiao MB, Ding Y. Modeling and compensation of hysteresis for pneumatic artificial muscles based on Gaussian mixture models. Sci China Technol Sci. 2019;62(7):1094–102. https://doi.org/10.1007/s11431-018-9488-1
20 Al-Ibadi A, Nefti-Meziani S, Davis S. The design, kinematics and torque analysis of the self-bending soft contraction actuator. Actuators. 2020;9(2):33. https://doi.org/10.3390/act9020033
21 Al-Mosawi HA, Al-Ibadi A, Abdalla TY. A comprehensive comparison of different control strategies to adjust the length of the soft contractor pneumatic muscle actuator. Iraqi J Electr Electron Eng. 2022;18(2):101–9. https://doi.org/10.37917/ijeee.18.2.13
22 Rihmi MK, Bintoro G, Rahman MA, Ali GP. Accuracy analysis of distance measurement using sonar ultrasonic sensor HC-SR04 on several types of materials. J Environ Eng Sustain Technol. 2024;11(1):10–3. https://doi.org/10.21776/ub.jeest.2024.011.01.2
23 Al-Ibadi A, Nefti-Meziani S, Davis S. Valuable experimental model of contraction pneumatic muscle actuator. In: Proceedings of the 21st International Conference on Methods and Models in Automation and Robotics (MMAR). IEEE; 2016. p. 744–9. https://doi.org/10.1109/MMAR.2016.7575229
24 Abu Mallouh M, Araydah WS, Jouda B, Al-Khawaldeh MA. Comparative modeling study of pneumatic artificial muscle using neural networks, ANFIS and curve fitting. In: Proceedings of the 9th International Conference on Automation, Robotics and Applications (ICARA). IEEE; 2023. p. 134–8. https://doi.org/10.1109/ICARA56516.2023.10125812